ELECTRONIC SUPPLEMENTARY INFORMATION

for

Protonation and axial ligation intervened fluorescent turn-off sensing of picric acid in freebase and tin(IV) porphyrins

Rahul Soman, Subramaniam Sujatha and Chellaiah Arunkumar*

Bioinorganic Materials Research Laboratory, Department of Chemistry, National Institute of Technology Calicut, Kozhikode, Kerala, India – 673 601.

E-mail: arunkumarc@nitc.ac.in

Contents

Fig. S9 ^{1}H NMR spectra of **6** (a) without PA, (b) with 1 equiv. of PA and (c) with 2 equiv. of PA in $CDCl_3$ at 298 K.

Fig. S10 Relative percentage contribution of various intermolecular interactions in **3**·4-NP, $\mathbf{5}^{2+}\cdot 2PA^{-}$, **6**·PA and **6**·2,4-DNP based on Hirshfeld surface analysis.

Table S1. Photophysical data of the porphyrins, **1**–**9** in $CHCl_3$ at 298 K.

Table S2. Quenching efficiencies and K_{SV} values of porphyrins.

Table S3. Fluorescence lifetime of porphyrins in the presence and absence of PA.

Table S4. Crystallographic data of porphyrins, **3**·4-NP, $\mathbf{5}^{2+}\cdot 2PA^{-}$, **6**·PA and **6**·2,4-DNP.

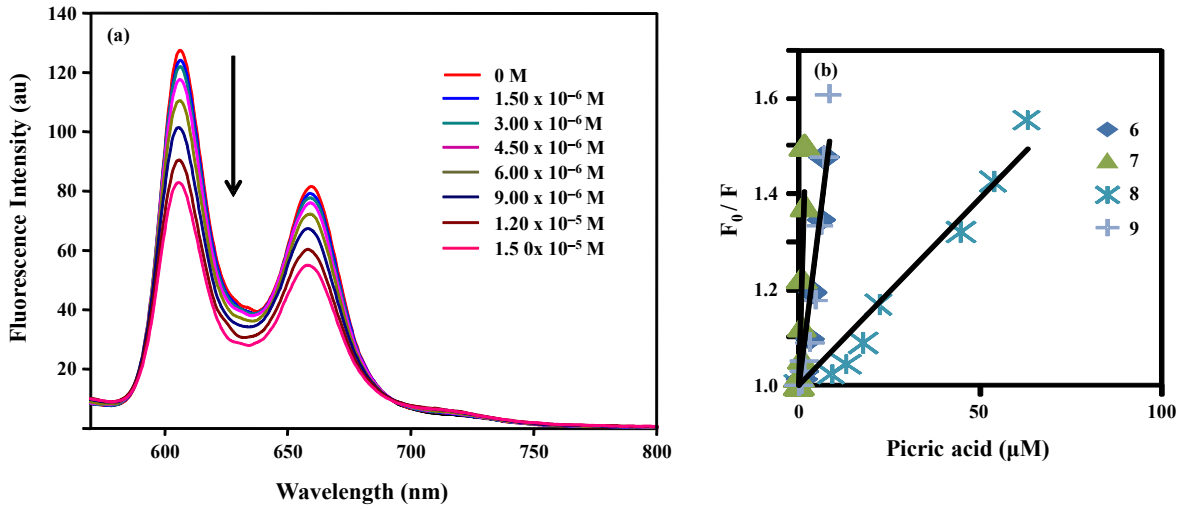

Fig. S1 (a) Fluorescence quenching of **6** (1 x 10^{-8} M in $CHCl_3$) upon incremental addition of PA (1.50 x 10^{-6} M in $CHCl_3$) (λ_{exc} = 426 nm); (b) Stern–Volmer plots for **6**–**9** against different concentrations of PA.

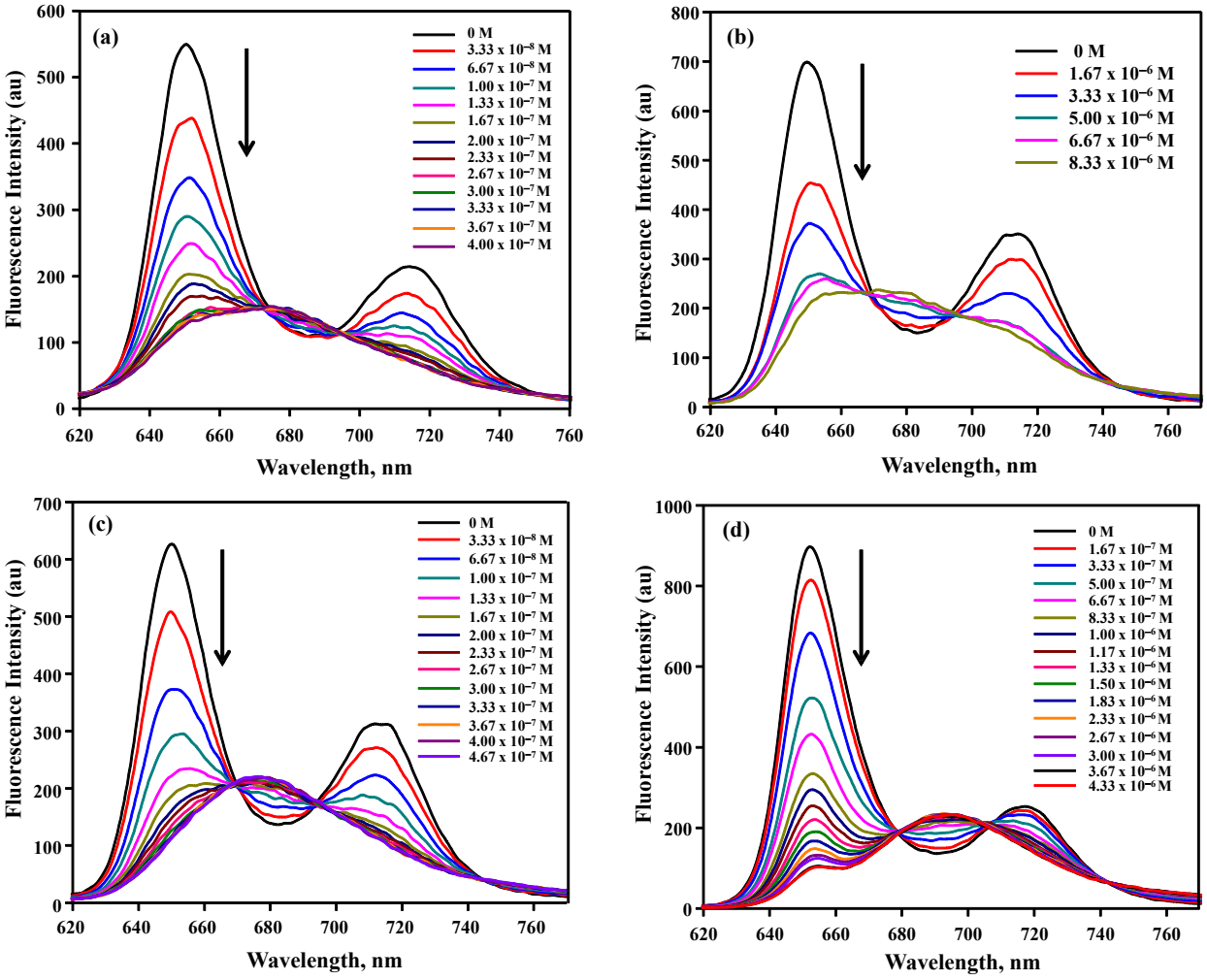

Fig. S2 Fluorescence quenching spectra of freebase porphyrins, (a) **1**; (b) **3**; (c) **4** and (d) **5** (~ 1 x 10^{-8} M in $CHCl_3$) upon incremental addition of PA (in $CHCl_3$) (λ_{exc} = 426 nm).

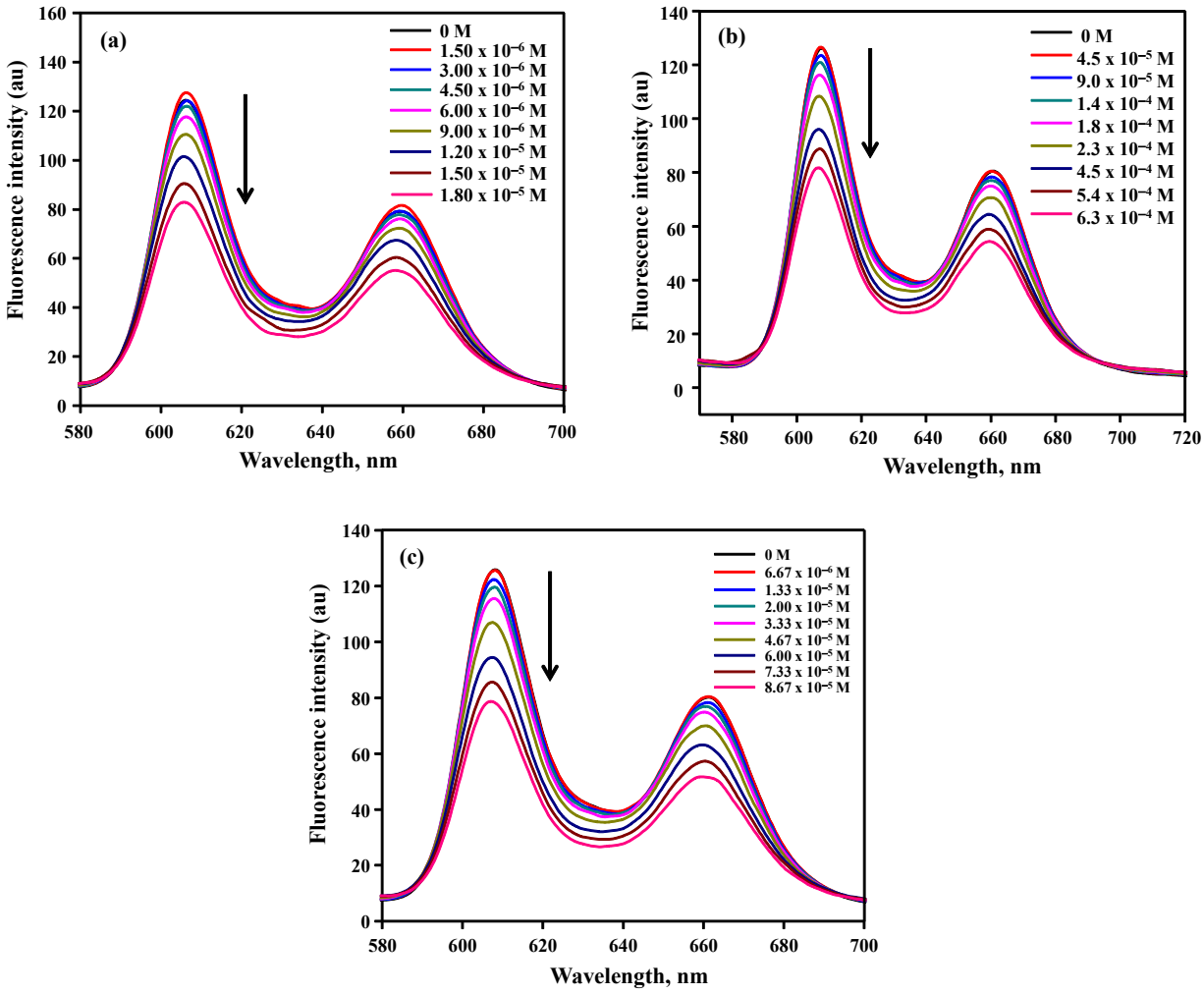

Fig. S3 Fluorescence quenching spectra of tin(IV) porphyrins, (a) **7**; (b) **8** and (c) **9** (~ 1 x 10^{-8} M in $CHCl_3$) upon incremental addition of PA (in $CHCl_3$) (λ_{exc} = 426 nm).

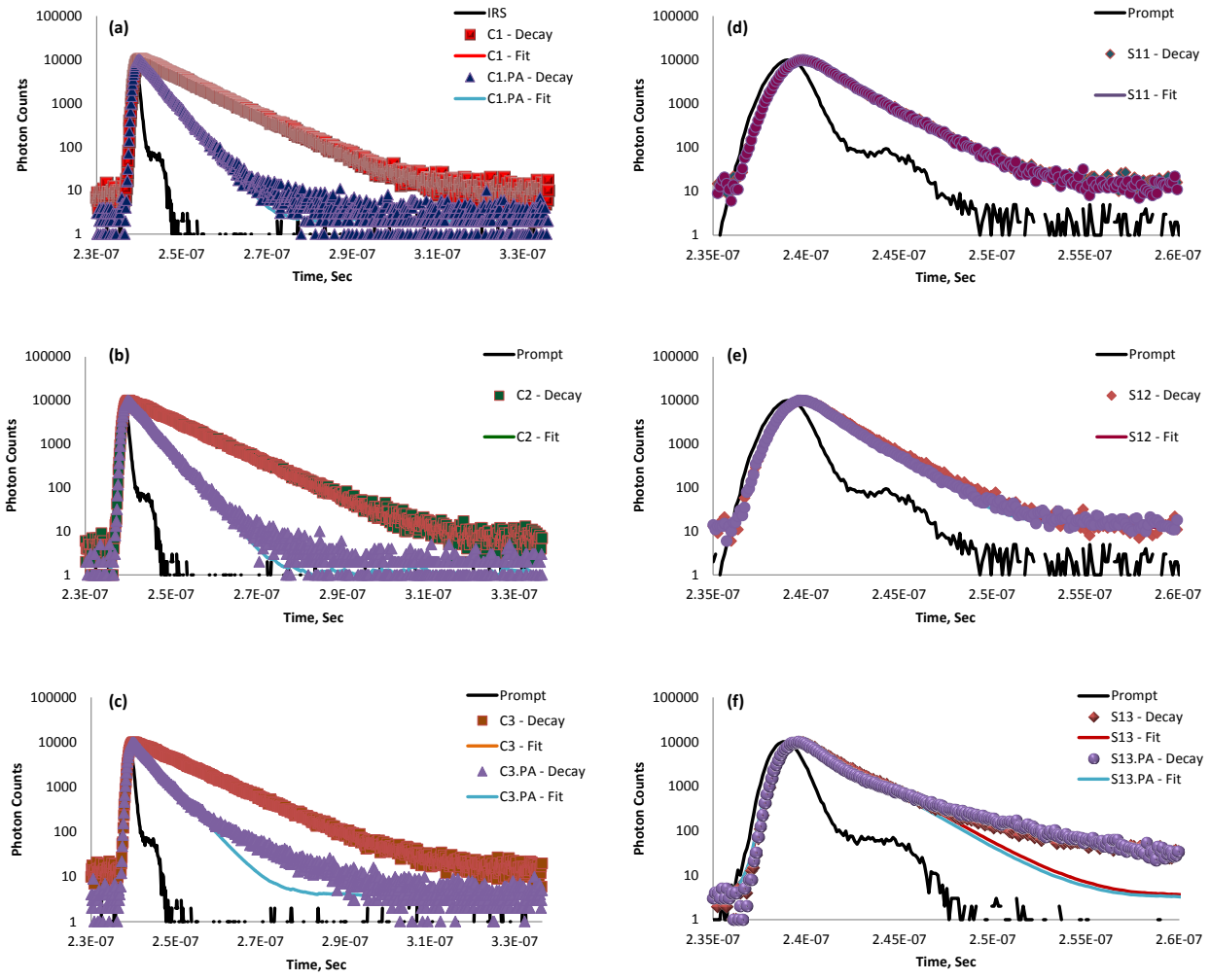

Fig. S4 Fluorescence decay curves of freebase, (a) **1**, (b) **2** and (c) **3** observed at 650 nm; tin(IV) porphyrins, (d) **6**, (e) **7** and (f) **8** observed at 600 nm along with IRF measured ($CHCl_3$) in the presence and absence of PA. (λ_{exc} = 460 nm).

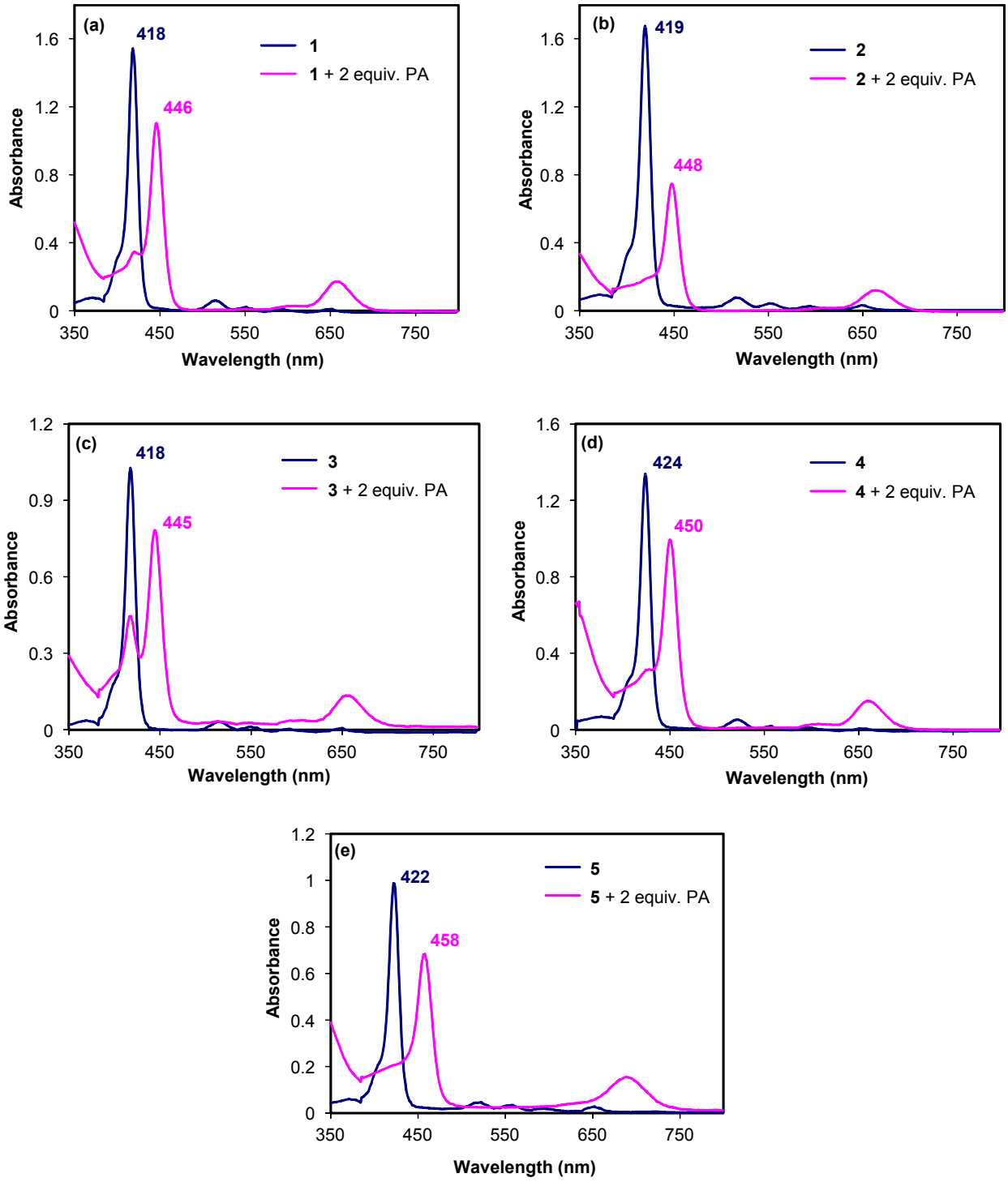

Fig. S5 (a) UV-visible spectra of (a) **1** with PA; (b) **2** with PA; (c) **3** with PA; (d) **4** with PA; and (e) **5** with PA.

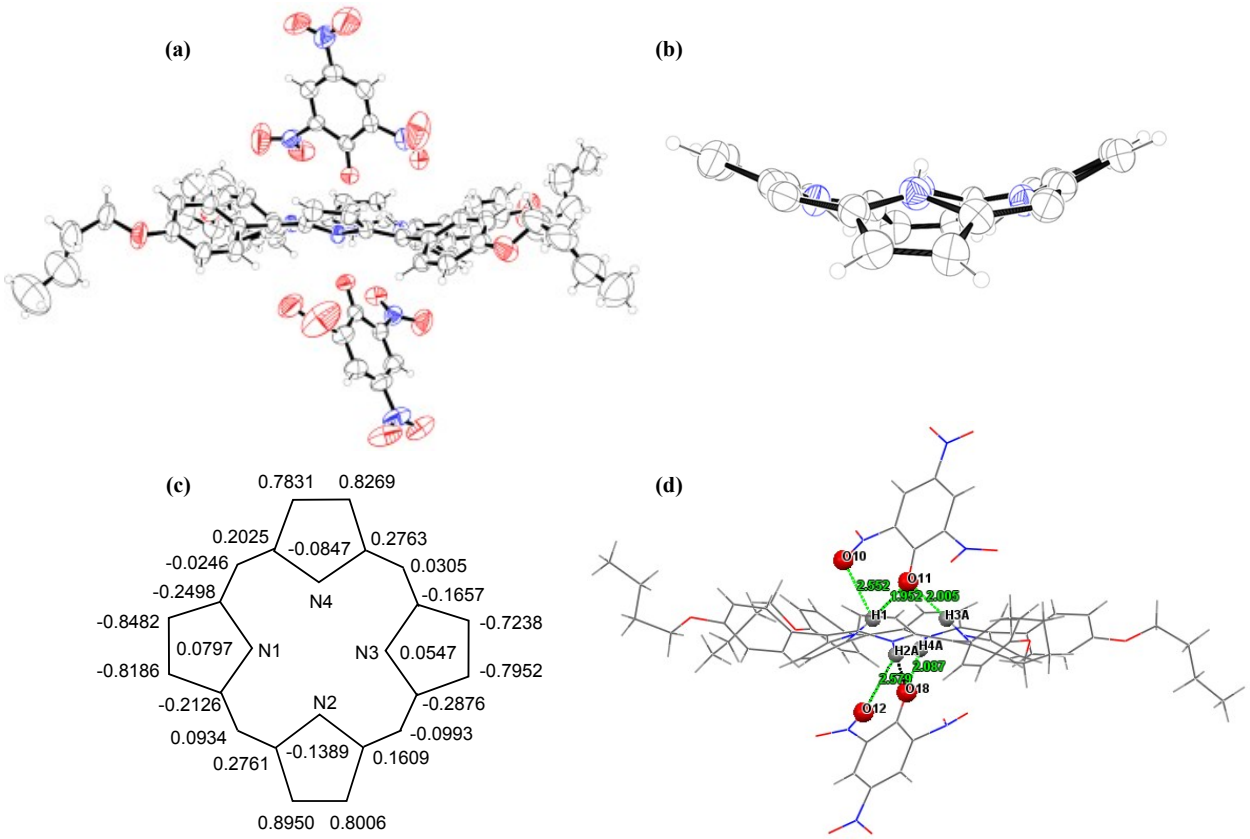

Fig. S6 ORTEP diagram of $\mathbf{5}^{2+}\cdot 2PA^{-}$ (a) top view, (b) side on view, (c) mean plane deviation of 24-atoms and (d) hydrogen bonding interactions between 2,4,6-trinitrophenolate and imino hydrogens (atoms involved in H-bonding interactions were represented as ball and sticks).

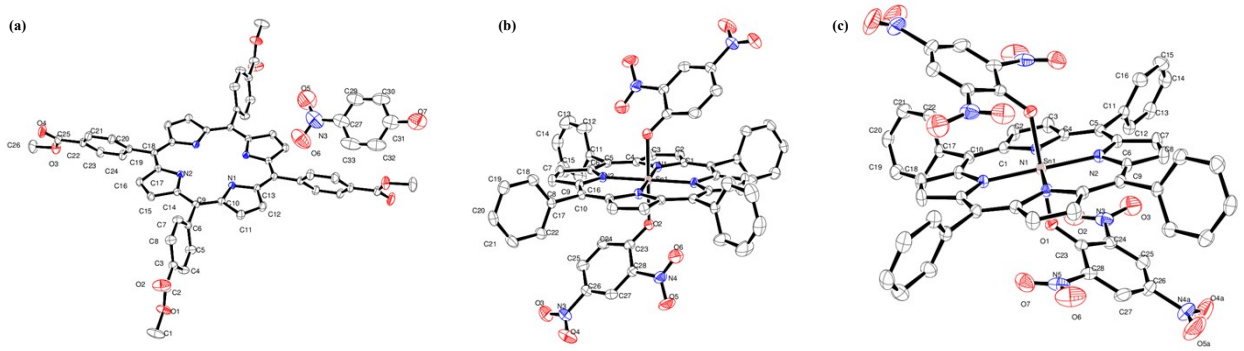

Fig. S7 ORTEP diagrams with labelling of atoms (hydrogens were omitted for clarity) of (a) **3**·4-NP, (b) **6**·2,4-DNP and (c) **6**·PA.

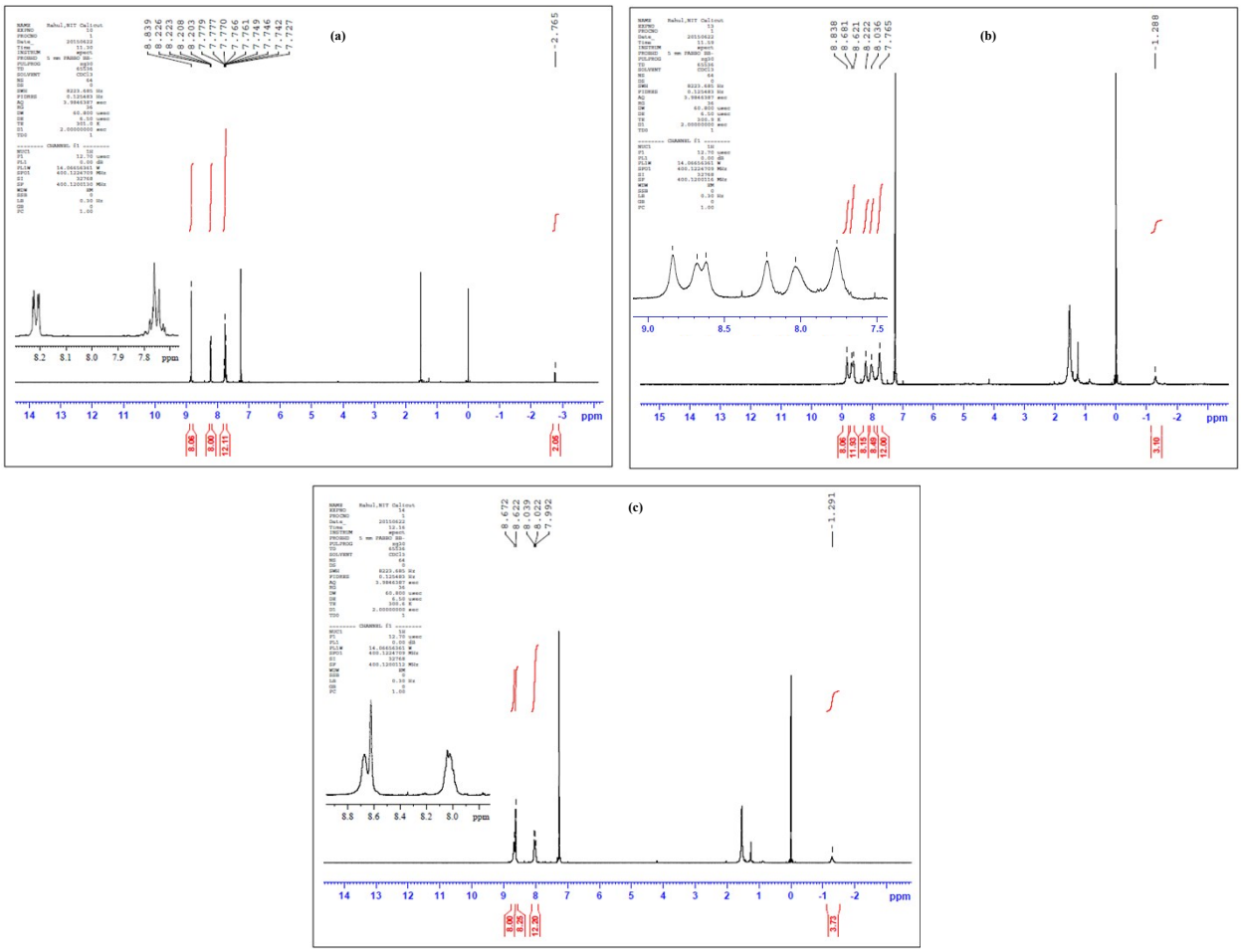

Fig. S8 ^{1}H NMR spectra of **1** (a) without PA, (b) with 1 equiv. of PA and (c) with 2 equiv. of PA in $CDCl_3$ at 298 K.

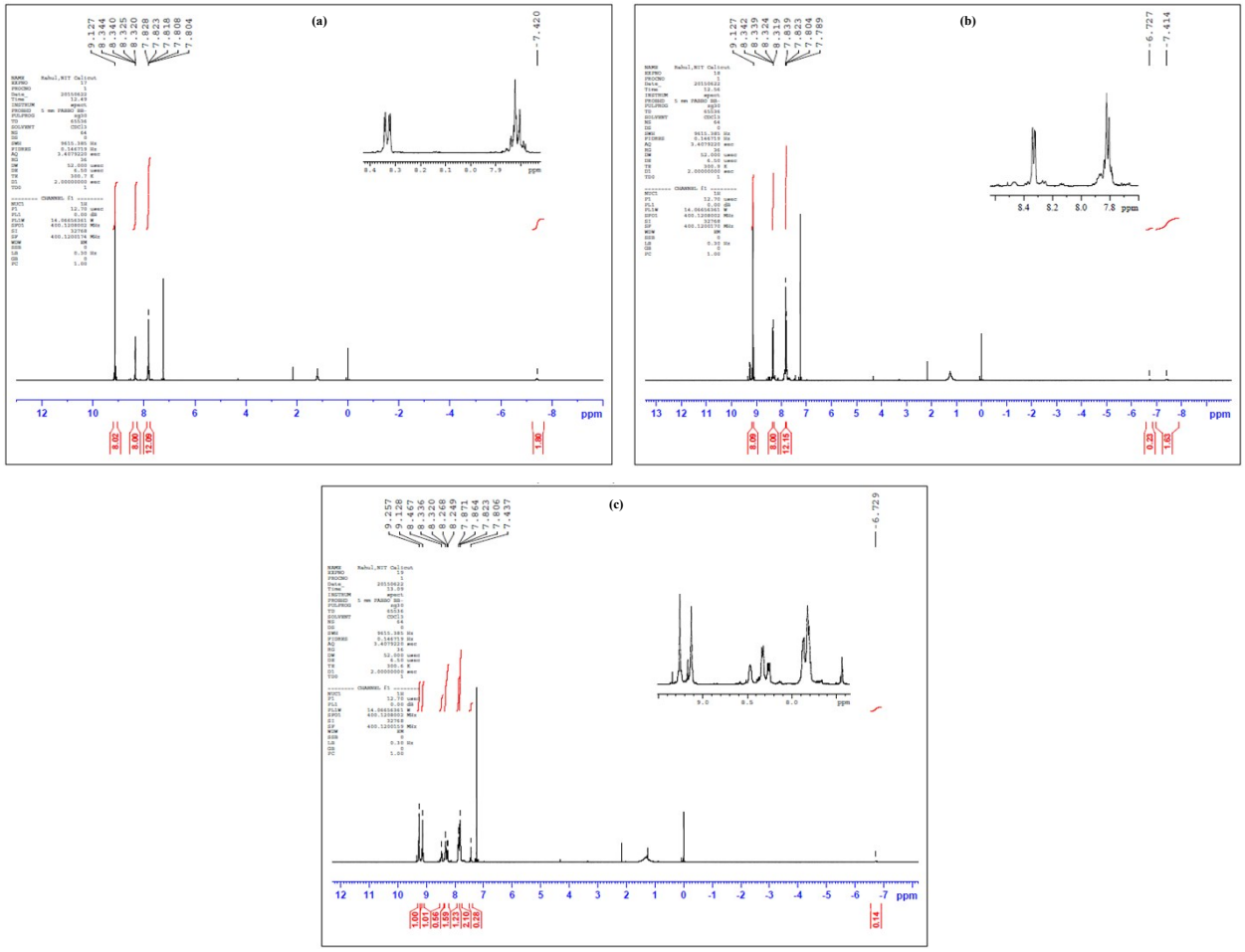

Fig. S9 ^{1}H NMR spectra of **6** (a) without PA, (b) with 1 equiv. of PA and (c) with 2 equiv. of PA in $CDCl_3$ at 298 K.

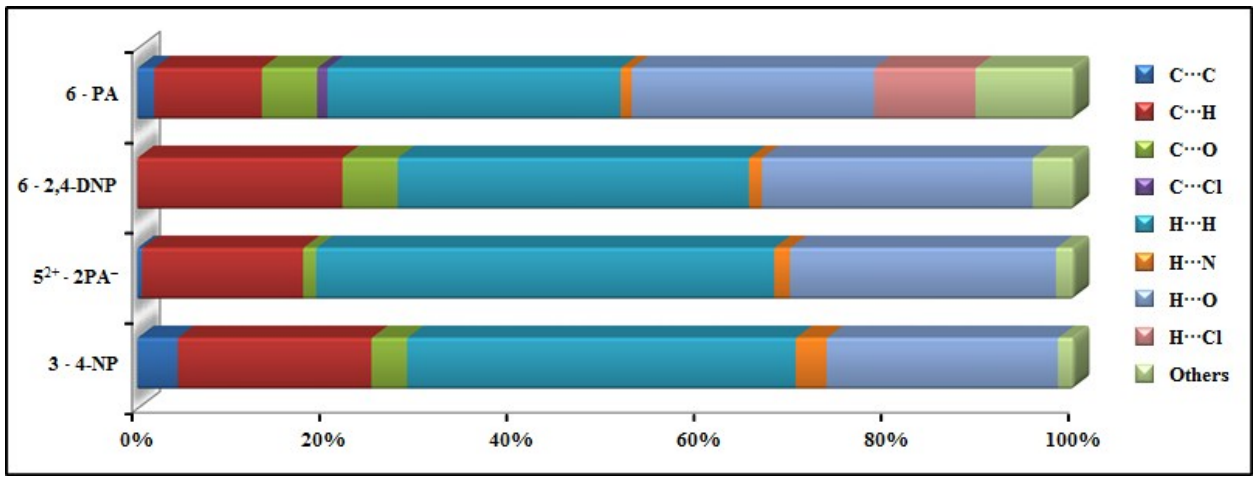

Fig. S10 Relative percentage contribution of various intermolecular interactions in **3**·4-NP, $\mathbf{5}^{2+}$·2PA^{-}, **6**·PA and **6**·2,4-DNP based on Hirshfeld surface analysis.

Table S1. Photophysical data of the porphyrins, **1**–**9** in $CHCl_3$ at 298 K.

Compound	Absorption maxima λ_{max}, nm (log ε)	Fluorescence emission maxima (λ_{max}, nm)[a]	Quantum Yield (Φ) (S_1-S_0)
1	419 (6.34), 514 (4.97), 548 (4.56), 591 (4.46), 648 (4.33)	439, 651, 716	0.11[b]
2	420 (6.29), 515 (4.91), 551 (4.62), 593 (4.38), 651 (4.38)	464, 653, 719	0.122
3	417 (6.12), 514 (4.88), 549 (4.50), 591 (4.33), 646 (4.12)	650, 716	0.057[c]
4	424 (6.18), 513 (5.10), 551 (4.68), 595 (4.78), 650 (4.19)	465, 656, 722	0.120
5	423 (6.09), 514 (5.03), 548 (4.49), 589 (4.60), 658 (4.19)	467, 656, 721	0.125
6	426 (6.11), 560 (4.72), 598 (4.43)	433, 603, 654	0.033
7	429 (6.17), 563 (4.97), 603 (4.90)	436, 608, 659	0.052
8	427 (5.97), 561 (4.89), 600 (4.76)[d]	462, 605, 657	0.017[c]
9	432 (5.95), 565 (4.54), 606 (4.50)	435, 607, 657	0.046

[a]Fluorescence spectra of porphyrins were obtained as a function of λ_{ex} in the Soret band region. [b]Taken from the ref. O. Ohno, Y. Kaizu, H. Kobayashi, *J. Chem. Phys.,* 1985, 82, 1779–1787. [c]Taken from the ref. R. Soman, D. Raghav, S. Sujatha, K. Rathinasamy, C. Arunkumar, *RSC Advances*, 2015, 5, 61103-61117. [d]THF as solvent.

Table S2. Quenching efficiencies and K_{SV} values of porphyrins.

Porphyrin	NACs	K_{SV} (M^{-1})	Quenching Efficiency (%)
1	PA	9.35×10^6	86
2	PA	3.90×10^7	90
3	PA	2.92×10^4	83
4	PA	1.93×10^6	85
5	PA	1.32×10^7	85
6	PA	6.63×10^3	65
7	PA	2.24×10^4	70
8	PA	7.80×10^2	34
9	PA	9.59×10^3	58
H_2OMP[a]	TNT	3.24×10^2	-
H_2OMP[a]	DNT	2.26×10^2	-
CdTPP- doped silica film[c]	TNT	-	56
Hg decorated porphyrin[b]	PA	1.6×10^7	94[d]
Hg decorated porphyrin[b]	DNP	4.16×10^4	71[e]

[a]Taken from ref. 17a; [b]Taken from ref. 17b; [c]Taken from ref. 17c
[d]LOD is 18 ppb; [e]LOD is 140 ppb

Table S3. Fluorescence lifetime of porphyrins in the presence and absence of PA.

Compound	Fluorescence lifetime, τ (ns) in absence of PA	Fluorescence lifetime, τ (ns) in presence of PA
1	9.53	3.66
2	9.25	3.55
3	10.16	4.11
6	1.58	1.57
7	1.40	1.40
8	1.80	1.74

Table S4. Crystallographic data of porphyrins, **3**·4-NP, $\mathbf{5}^{2+}\cdot 2PA^{-}$, **6**·PA and **6**·2,4-DNP.

	3·4-NP	$\mathbf{5}^{2+}\cdot 2PA^{-}$	**6**·PA	**6**·2,4-DNP
Empirical formula	$C_{64}H_{50}N_6O_{14}$	$C_{72}H_{68}N_{10}O_{18}$	$C_{57}H_{33}Cl_3N_{10}O_{14}Sn$	$C_{56}H_{34}N_8O_{10}Sn$
fw	1127.10	1361.36	1306.97	1097.60
CCDC no.	980779	1058018	974216	1058017
Colour	black	purple	purple	purple
Crystal system	monoclinic	orthorhombic	monoclinic	triclinic
Space group	C2/c	$P\ 2_1\ 2_1\ 2_1$	C2/c	P -1
a, Å	32.538(2)	17.9987(14)	22.531	10.8117(3)
b, Å	7.1831(4)	18.3601(12)	9.691	11.0391(8)
c, Å	23.8130(18)	20.6419(16)	26.753	11.7580(5)
α, (deg)	90.00	90	90.00	102.915(2)
β, (deg)	99.118(5)	90	113.96	111.599(2)
γ, (deg)	90.00	90	90.00	105.250(2)
Volume ($Å^3$)	5495.3(7)	6821.3(9)	5338.1	1175.85(11)
Z	4	4	4	1
D_{calcd} (mg/m^3)	1.362	1.326	1.626	1.550
λ, Å	0.71073	0.71073	0.71073	0.71073
T (K)	296(2)	296(2)	296(2)	296(2)
No. of unique reflections	6728	12012	4654	4102
No. of parameters refined	390	1026	426	378
GOF on F^2	1.058	1.024	0.949	1.061
R_1[a]	0.0687	0.0690	0.0354	0.0284
wR_2[b]	0.1884	0.1786	0.0836	0.0749

[a] $R_1 = \Sigma||F_o|-|Fc||/\Sigma|F_o|$; $I_o > 2\sigma(I_o)$. [b] $wR_2 = [\Sigma\, w(F_o^2-F_c^2)^2/\Sigma w(F_o^2)^2]^{1/2}$.